ASTRONOMY & ASTROPHYSICS
SUPPLEMENT SERIES

JANUARY II **2000**, PAGE 193

Astron. Astrophys. Suppl. Ser. **141**, 193–209 (2000)

Dense molecular gas in Seyfert galaxies⋆

S.J. Curran, S. Aalto, and R.S. Booth

Onsala Space Observatory, Chalmers University of Technology, S-439 92 Onsala, Sweden
e-mail: sjc@oso.chalmers.se

Received March 2; accepted October 22, 1999

Abstract. We have used the 20 m Onsala and 15 m SEST telescopes to observe the CO $J = 1 \rightarrow 0$ (simultaneously with CO $J = 2 \rightarrow 1$ at SEST) and HCN $J = 1 \rightarrow 0$ (simultaneously with CS $J = 3 \rightarrow 2$ at SEST) transitions in 20 Seyfert galaxies. The sample consists of the 18 galaxies detected in CO $J = 1 \rightarrow 0$ by Heckman et al. (1989) plus 2 which were not detected in their survey. We have successfully detected all of the galaxies in the CO transition and 13 in HCN of which NGCs 1667, 2273, 5033, 5135, 6814 and Mrk 273 are new detections. For the galaxies in which the beam-width exceeds ≈ 10 kpc we find that $\frac{L_{\rm HCN}}{L_{\rm CO}} \approx 1/6$, i.e. a global ratio similar to that of ultra-luminous infrared galaxies and over 10 times the ratio for normal spiral galaxies. This implies that $\frac{L_{\rm FIR}}{L_{\rm CO}}$ ($L_{\rm FIR} \sim 10^{11}\ L_{\odot}$ Seyferts) $\approx 10\frac{L_{\rm FIR}}{L_{\rm CO}}$ (normal spirals) and we believe that the far infrared fluxes in our sample arise from star-burst activity, although we cannot rule out the possibility of a contribution from active galactic nuclei.

Key words: galaxies: Seyfert–galaxies: abundances — galaxies: ISM

1. Introduction

Activity in the centres of galaxies ranges from extremely compact active galactic nuclei (AGN) powered by mass accretion onto a black hole (Begelman et al. 1984; Rees 1984) to extended star-bursts of more modest power. In some extreme ultra-luminous infrared galaxies (ULIRGs)[1], e.g. in Arp 220 the star-powered luminosity may rival that of a compact AGN. Interest in the connection between the star-burst phenomenon and the central AGN has been stimulated by the fact that in galaxies with dominant AGNs, there may be significant amounts of circumnuclear gas, e.g. NGC 1068 (e.g. Tacconi et al. 1994) and Centaurus A (e.g. Rydbeck et al. 1993). Gas fuels the star-forming activity and responds both physically and chemically to the ultraviolet radiation and supernovae produced in a young population of massive stars. Dynamically, gas clouds are highly dissipative, relative to the stars and thus sink readily towards the centres of galactic gravitational potentials, possibly fuelling the black hole. Indeed, recent VLBI observations of molecular masers (e.g. NGC 4258) have revealed a very close connection between molecules and accretion discs surrounding galactic black holes Miyoshi et al. 1995. Also, recent interferometric observations of the type 2 Seyfert galaxy NGC 1068 have shown that the HCN gas is much more confined than the CO (e.g. Tacconi et al. 1996), and all interferometric studies (e.g. Helfer & Blitz 1997) show the HCN to be mainly concentrated towards the centre. We are therefore confident that the HCN emission will trace gas in the nuclear regions. In addition to this, Solomon et al. (1992) (hereafter SDR92) suggest, from their HCN observations, that (galactic) IR luminosities are a consequence of star formation, rather than of an AGN. In order to compare how Seyferts differ from non-Seyferts in their gas content, we investigate the CO, HCN and infrared luminosities of the 18 galaxies detected in CO $1 \rightarrow 0$ by Heckman et al. (1989) with the NRAO 12 m. We chose to observe these galaxies because:

1. They form a good sample of Seyfert galaxies;
2. To verify the results of Heckman et al. (1989), who find higher molecular gas abundances in type 2 than in type 1 Seyferts. This issue is addressed in Curran (2000a).

Send offprint requests to: S. Curran

⋆ Based on results collected at the European Southern Observatory, La Silla, Chile and Onsala Space Observatory, Sweden.

[1] Where the far infrared luminosities of $L_{\rm FIR} > 10^{11}\ L_{\odot}$ give FIR to molecular gas luminosity ratios which are an order of magnitude higher than for normal spiral galaxies Soifer et al. 1984; Sanders et al. 1986; Solomon & Sage 1988).

Table 1. Beam sizes and efficiencies

Transition	ν [GHz]	HPBW [″]		$\eta_{\rm mb}$	
		OSO	SEST	OSO	SEST
HCN $1 \rightarrow 0$	89	44	57	0.59	0.75
CO $1 \rightarrow 0$	115	33	45	0.50	0.70
CS $3 \rightarrow 2$	147	–	34	–	0.66
CO $2 \rightarrow 1$	230	–	22	–	0.50

In addition to these results, in this paper we also present the CO $2 \rightarrow 1$ and CS $3 \rightarrow 2$ results from the Southern part of this sample.

2. Observations

We have observed the CO $1 \rightarrow 0$ (115 GHz) and HCN $1 \rightarrow 0$ (88.6 GHz) lines in a sample of 20 Seyfert galaxies. The Southern sample was observed in December 1997 and October 1998 with the 15 m SEST[2] at La Silla, Chile. Since the 100 GHz and 115 GHz can be used simultaneously with the 150 GHz and the 230 GHz receivers, respectively, we also observed CS $3 \rightarrow 2$ (147 GHz) and CO $2 \rightarrow 1$ (230 GHz). All receivers were tuned to the single-band mode and typical system temperatures, on the $T_{\rm A}^*$-scale, were 150 K at 89 GHz, 200 to 300 K at 115 GHz, 200 K at 150 GHz and 300 K at 230 GHz. The HPBWs are 57″, 45″, 34″, and 22″, respectively. The backends were acousto-optical spectrometers with 1440 channels and a channel width of 0.7 MHz. We used dual-beam switching with a throw of about 12′ in azimuth, with pointing errors being typically 3″ rms on each axis. The intensity was calibrated using the chopper-wheel method. For the first observing run the weather was excellent, and only the removal of linear baselines was required. However, two of the sources, NGCs 6814 and 7130, were within the sun-limit and, after the application for more time, were observed during the second run under similarly good conditions.

The Northern sample was originally observed in February 1998 with the 20 m telescope at Onsala Space Observatory (OSO). During this session, however, the weather was unfavourable and more time was awarded for the following November. Both the CO $1 \rightarrow 0$ and HCN $1 \rightarrow 0$ transitions were observed with the SIS 100 GHz receiver. The HPBWs are 33″ and 44″, respectively. The backend was a filter-bank with a bandwidth of 512 MHz and a channel separation of 1 MHz. We used a similar dual-beam switching as the SEST observations and obtained similar pointing errors. Although far from ideal for most of the session, the weather was a great improvement over the previous run, with HCN being observed when the weather was poorest. Typical system temperatures were around 500 K for CO. This is considerably worse than the optimal 300 K, but given the improved receivers, is comparable with the system temperatures of Heckman et al. (1989). Some of the Northern sources were re-observed in April 1999 when the excellent weather gave system temperatures of $\approx$ 230 K and $\approx$ 350 K for the HCN and CO lines, respectively. As with the SEST data, only linear baselines were removed.

[2] The Swedish-ESO Sub-millimetre Telescope is operated jointly by ESO and the Swedish National Facility for Radio Astronomy, Onsala Space Observatory, Chalmers University of Technology.

3. Results

Upon comparison of the CO detections (Figs. 1 and 2) with those from previous surveys (Heckman et al. 1989; Maiolino et al. 1997; Papadopoulos & Seaquist 1998), we find that, for the most part, we have similar results with the following exceptions: CO $1 \rightarrow 0$ in NGC 1365 is similar to that of Maiolino et al. (1997); Papadopoulos & Seaquist (1998), although more symmetric than the detection of Heckman et al. (1989). Our $2 \rightarrow 1$ detection is not as symmetric as that of Papadopoulos & Seaquist (1998) and since the profile of Sandqvist et al. (1995) is also quite symmetrical we attribute our asymmetry to a pointing error. In NGC 1667 the profile is identical in shape to that of Heckman et al. (1989) but reflected with the peak occurring at the minimum, as opposed maximum velocity. In the case of Maiolino et al. (1997); Papadopoulos & Seaquist (1998), the peak also occurs at the maximum although these are somewhat more symmetric, indicating that we have a pointing error. NGC 5033; our detection appears to be somewhat skewed compared with those of Heckman et al. (1989); Maiolino et al. (1997); Papadopoulos & Seaquist (1998), although of a similar integrated intensity. NGC 5548; undetected by Heckman et al. (1989) and not observed by Papadopoulos & Seaquist (1998), our detection has a somewhat wider profile than that of Maiolino et al. (1997). The results of the observations are summarised in Table 2[3], where the upper limits for HCN $1 \rightarrow 0$ and $3 \rightarrow 2$ are over the velocity range of the CO $1 \rightarrow 0$ detections.

The luminosities according to the integrated intensity over the projected beam area are shown in Table 3[4].

Testing our global results, initially we obtained a fair linear fit by plotting $\ln L_{\rm CO}$ against $\ln L_{\rm HCN}$ for the sample galaxies with recessional velocities exceeding 4000 km s^{-1}. This corresponds to a HPBW of $\approx$ 12 kpc (at SEST,

[3] $I_{\rm mb} = I_{\rm A}^*/\eta_{\rm mb}$, where $I_{\rm A}^*$ is the velocity integrated Rayleigh-Jeans antenna temperature above the atmosphere and $\eta_{\rm mb}$ is the measured main-beam efficiency of the telescope.

[4] Again Sy refers to the Seyfert type but here and in Table 4 we use the classification scheme of Meurs & Wilson (1984); Edelson (1987); Osterbrock & Shaw (1988); Heckman et al. (1989); Maiolino & Rieke (1995) where types 1, 1.2 and 1.5 constitute type 1 Seyferts and types 1.8, 1.9 and 2 constitute type 2 Seyferts.

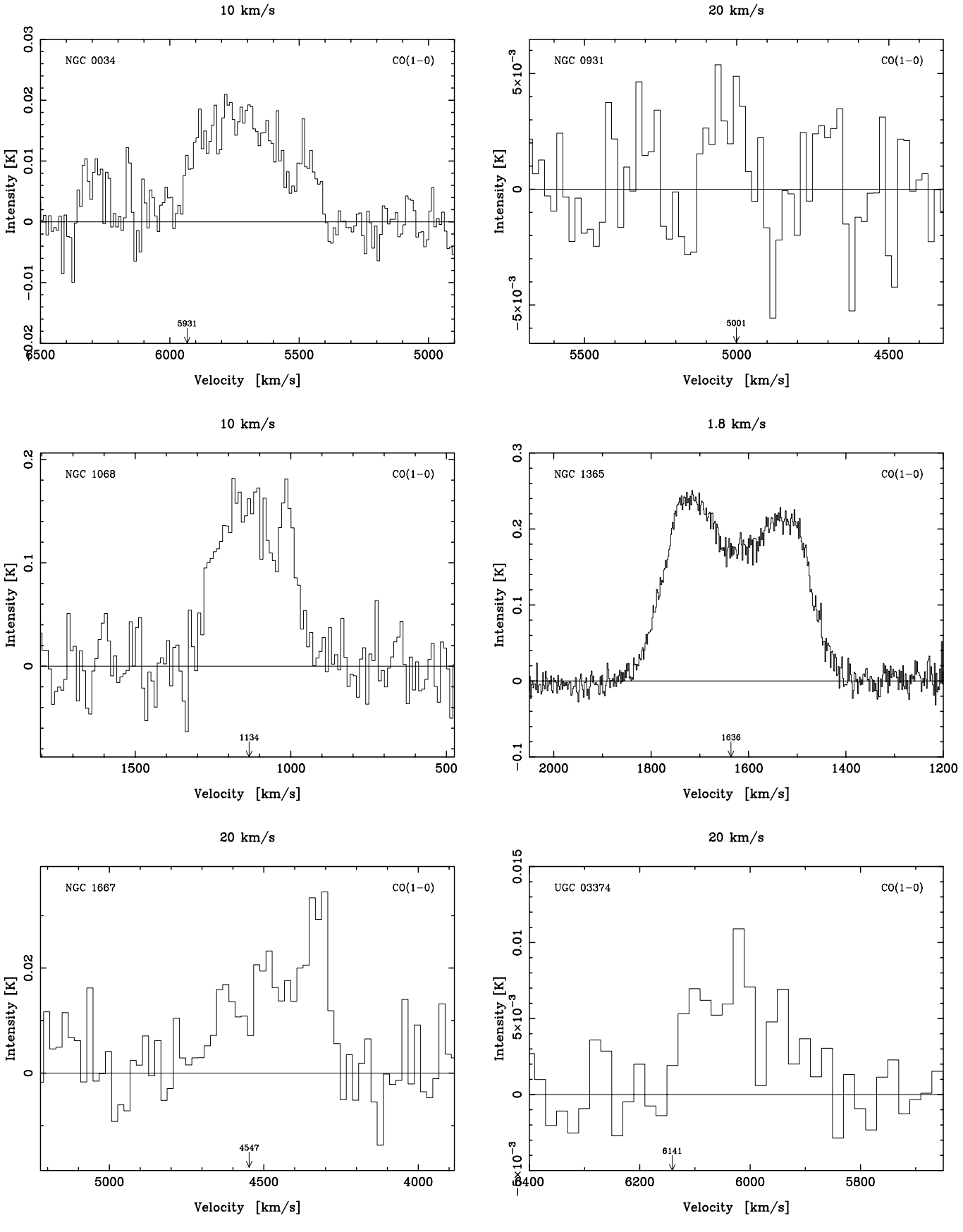

Fig. 1. The CO $J = 1 \rightarrow 0$ results. Here and in Figs. 2, 3 and 4 the intensity scale is $T_{\rm A}^{*}$ and the velocity resolution is shown above each scan

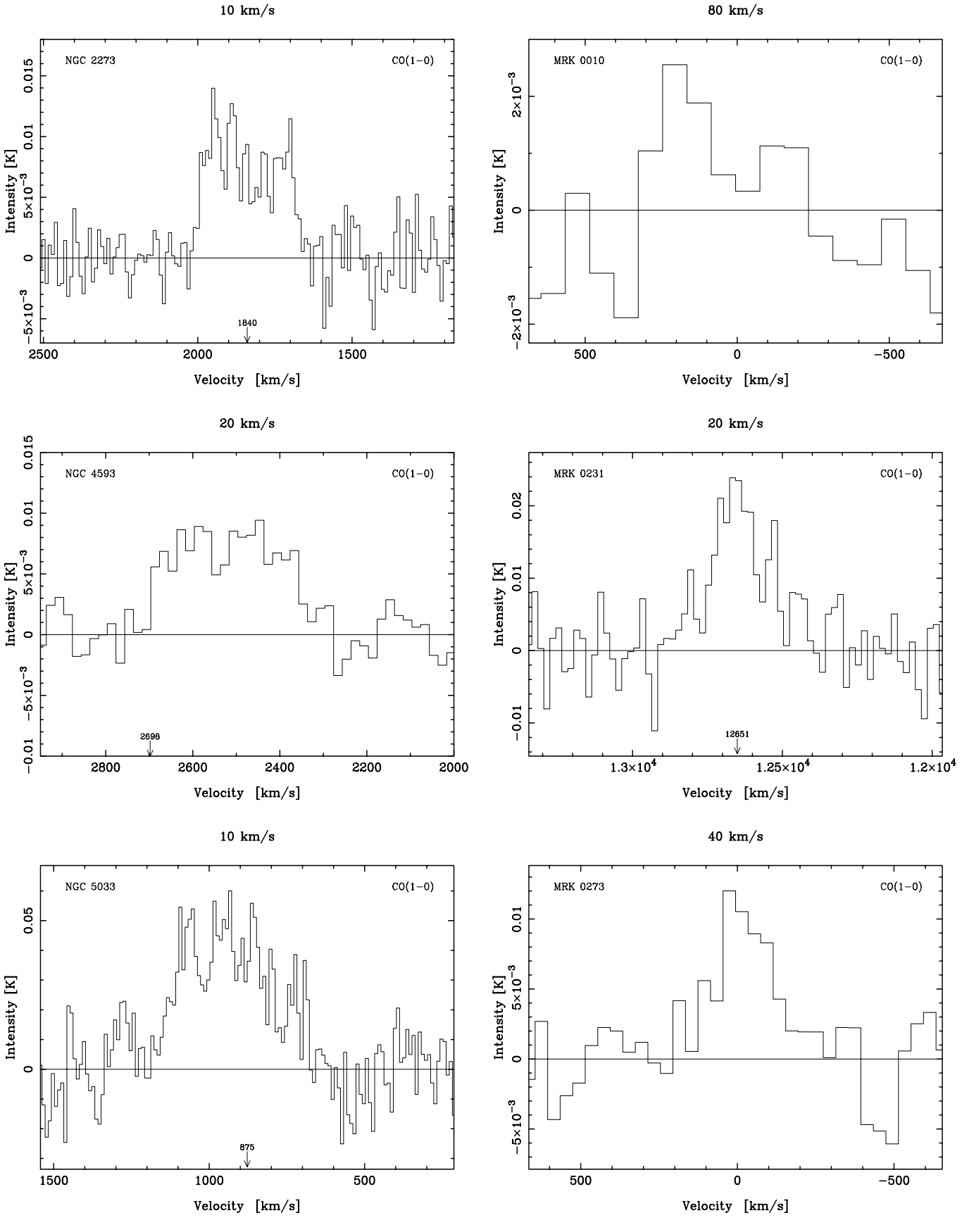

Fig. 1. continued

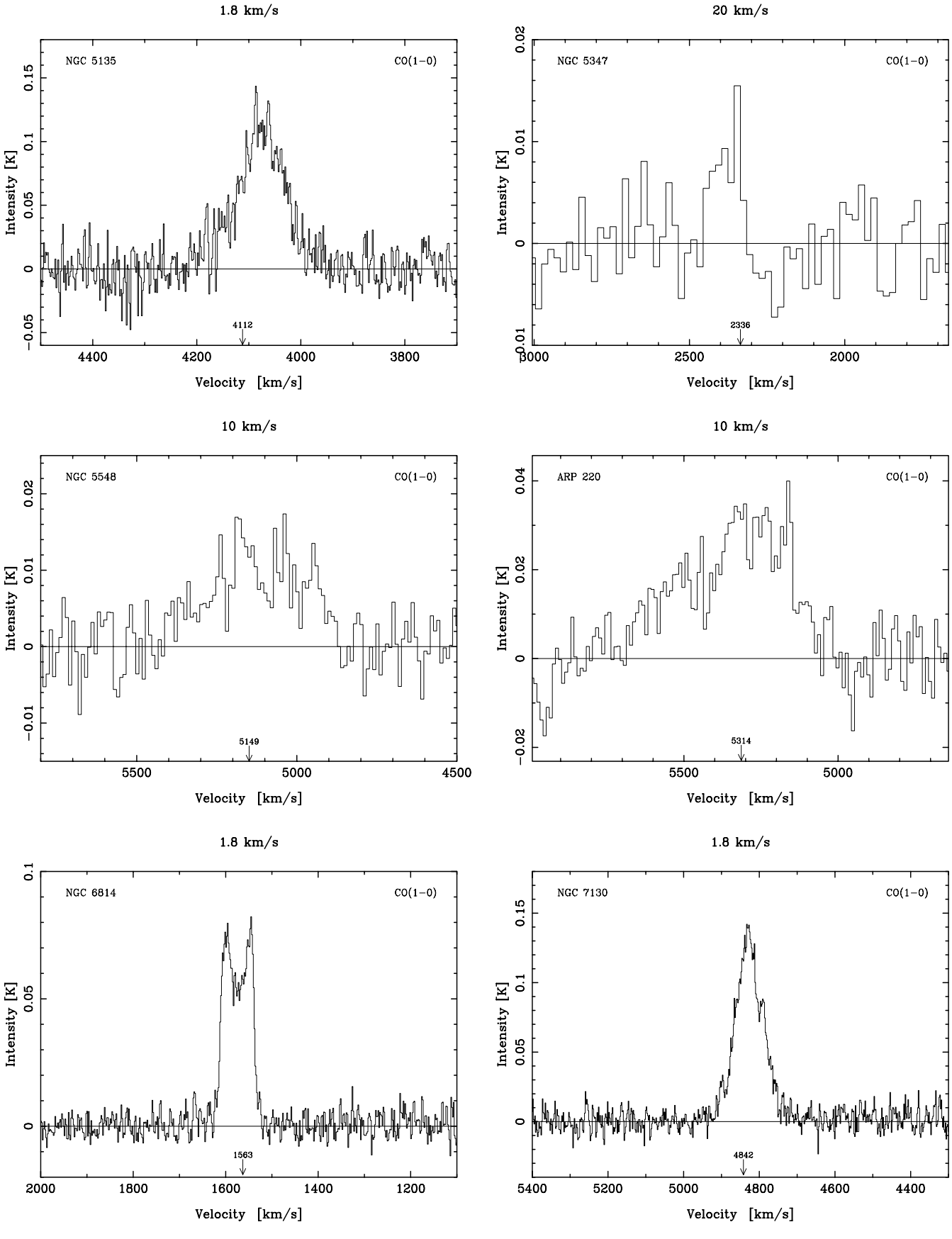

Fig. 1. continued

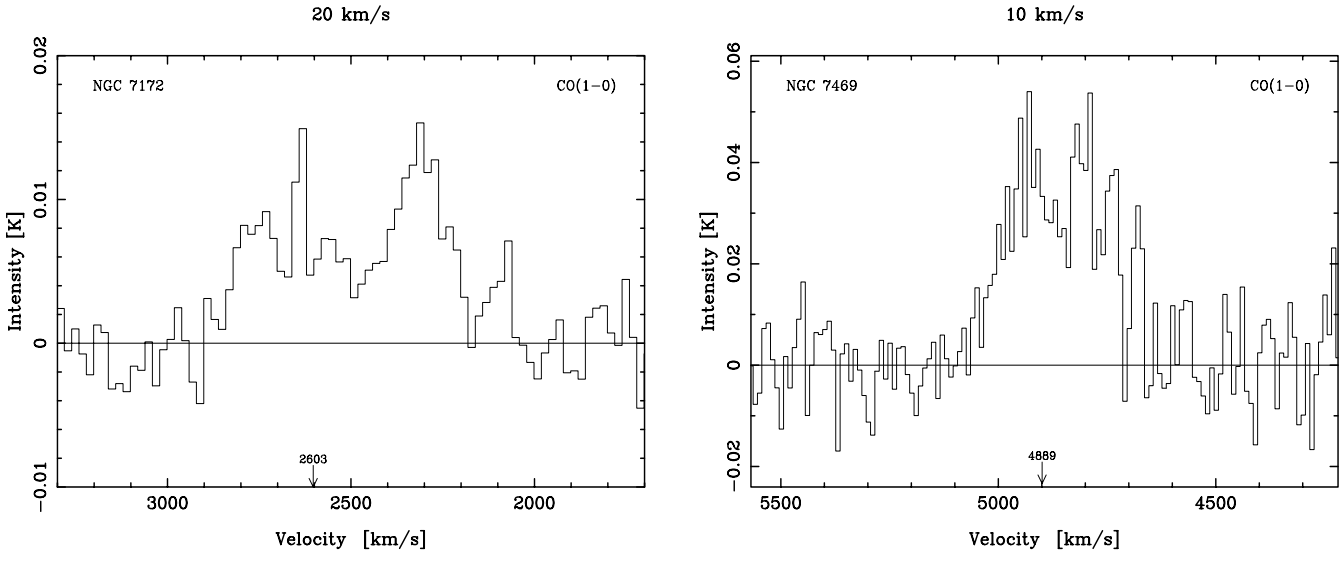

Fig. 1. continued

Table 2. The 18 Seyfert galaxies detected in CO $1 \rightarrow 0$ by Heckman et al. (1989) hbw+89 plus two non-detections (†, selected in order to provide a more balanced sample of type 1 and type 2 Seyferts) which are observable from OSO and SEST (Teles.). In this table Sy refers to the (intermediate; Osterbrock 1981) Seyfert type and v is the heliocentric radial velocity (NASA/IPAC Extragalactic Database). The final columns refer to the main-beam brightness temperature, $I_{\rm mb}$, [K km s^{-1}] measured for the corresponding transition, where the results have been rounded to two figures (because of $\eta_{\rm mb}$) and the errors and upper limits are according to 1σ (defined by the noise). The "New" column indicates whether these are first time detections in the HCN $1 \rightarrow 0$ transition for these galaxies

Galaxy	Sy	v [km s^{-1}]	Teles.	CO $1 \rightarrow 0$	CO $2 \rightarrow 1$	HCN $1 \rightarrow 0$	New	CS $3 \rightarrow 2$
NGC 0034	2	5931	SEST	10(1)	18(1)	1.6(0.2)		< 1
NGC 0931	1.5	5001	OSO	0.5(0.4)	–	< 0.8		–
NGC 1068	2	1134	OSO	86(3)	–	11(1)		–
NGC 1365	1.8	1636	SEST	97(1)	110(1)	6.0(0.1)		6.3(0.3)
NGC 1667	2	4547	OSO	15(1)	–	3.5(0.5)	$\surd$	–
UGC 03374/MCG 08-11-011	1.5	6141	OSO	2.8(0.3)	–	< 0.2		–
NGC 2273	2	1840	OSO	3.2(0.3)	–	0.5(0.3)	$\surd$	–
Mrk 10/UGC 04013	1	8770	OSO	1.0(0.3)	–	< 0.3		–
NGC 4593†	1	2698	SEST	1.7(0.4)	2.2(0.3)	–		–
Mrk 231/UGC 08058	1	12651	OSO	10(1)	–	1.0(0.2)		–
NGC 5033	1.9	875	OSO	32(2)	–	1.7(0.3)	$\surd$	–
Mrk 273/UGC 08696	2	11318	OSO	5(1)	–	3(1)	$\surd$	–
NGC 5135	2	4112	SEST	18(1)	25.8(0.6)	0.65(0.07)	$\surd$	< 1
NGC 5347	2	2336	OSO	1.3(0.5)	–	< 0.3		–
NGC 5548†	1.5	5149	SEST	2.4(1.2)	7.0(0.4)	–		–
Arp 220	2	5314	OSO	12(1)	–	2.4(1.0)		–
NGC 6814	1.5	1563	SEST	7.2(0.1)	3.9(0.1)	0.45(0.08)	$\surd$	< 1
NGC 7130/IC 5135	2	4842	SEST	17(1)	26(1)	0.7(0.1)		< 1
NGC 7172	2	2603	SEST	5.1(0.9)	7.3(0.3)	–		–
NGC 7469	1.2	4889	OSO	22(1)	–	1.7(0.4)		–

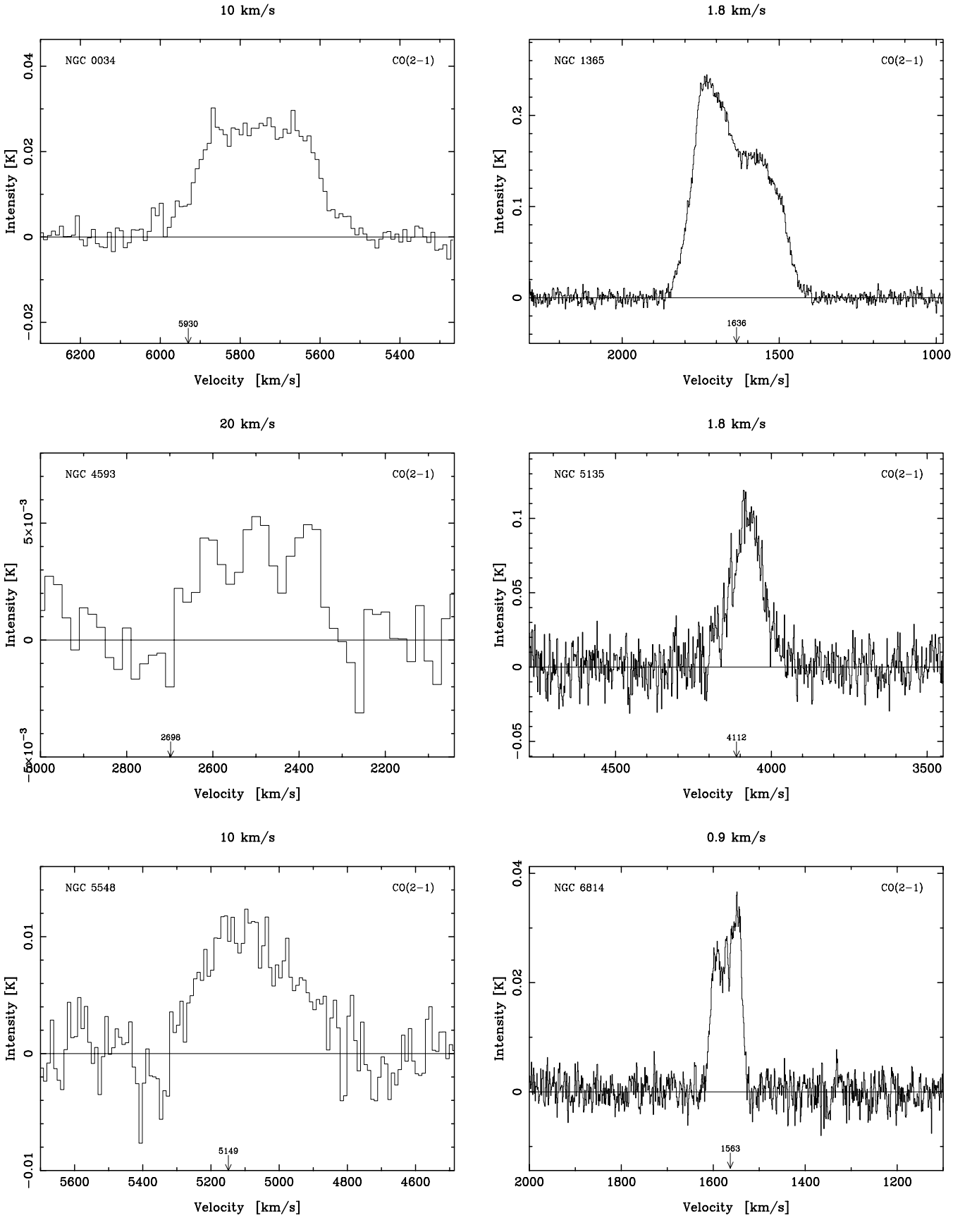

Fig. 2. The CO $J = 2 \rightarrow 1$ results

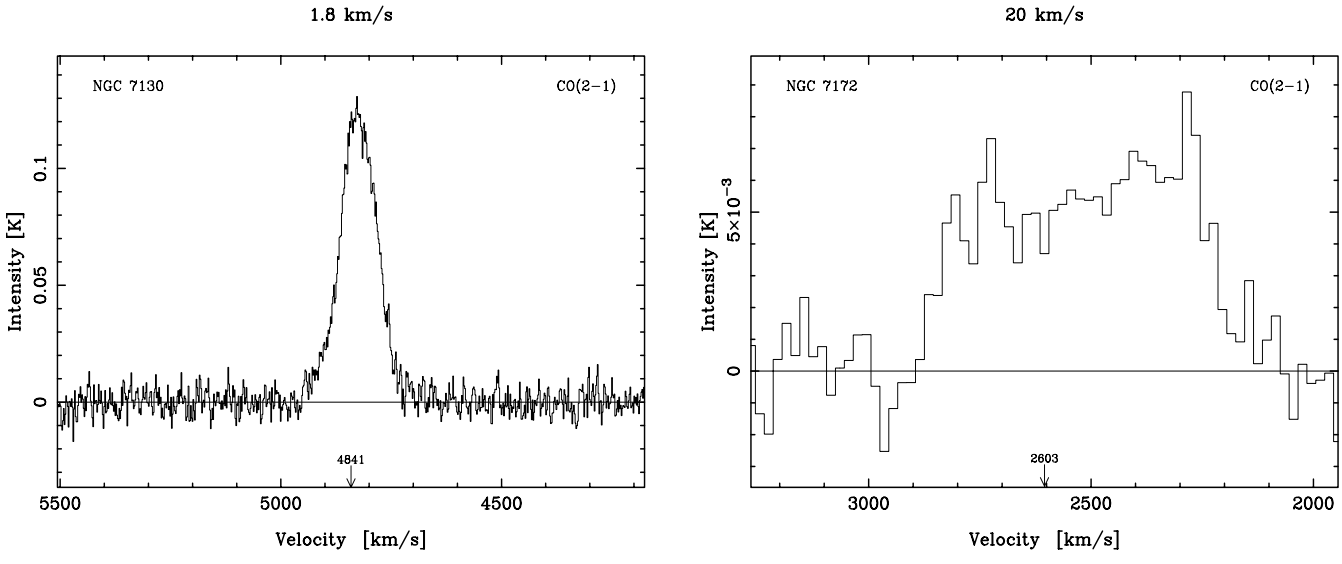

Fig. 2. continued

Table 3. The observed luminosities of the sample. $L_{\rm CO\ 1\rightarrow0}$, $L_{\rm CO\ 2\rightarrow1}$, $L_{\rm HCN\ 1\rightarrow0}$ and $L_{\rm CS\ 3\rightarrow2}$ refer to the luminosity over the HPBW for each respective transition, again with 1σ errors and upper limits [$\times10^3$ K km s^{-1} kpc^2]. Like Heckman et al. (1989) we have calculated the physical beam area by using the distances given by heliocentric radial velocities (Table 2) and assuming the same Hubble parameter as before, except in the case NGC 1365 where the assumed distance of 20 Mpc, to the Fornax cluster, is used. The $\int L_{\rm CO\ 1\rightarrow0}$ refers to the global CO $1\rightarrow0$ luminosity [$\times10^3$ K km s^{-1} kpc^2]: [a]Planesas, Gomez-Gonzalez & Martin-Pintado (1989) (over a partial map spanning ($120'' \times 120''$), [b]Young et al. (1995), [c]Sandqvist et al. (1995) (over $204'' \times 164''$) and [d]Bryant & Scoville (1996). Although apparently high, the CO luminosity in NGC 1068 (Young et al. 1995) is similar to that obtained from a large scale map of the Circinus galaxy (Curran 2000b; Curran et al. 2000). $L_{\rm FIR}$ [10^{10} $L_\odot$] refers to the far infrared luminosity computed using the FIR flux (Lonsdale et al. 1985; Heckman et al. 1989). The CO $2\rightarrow1$ (CO intensity ratios) and CS results are discussed in Curran (2000b)

Galaxy	Sy	$L_{\rm CO\ 1\rightarrow0}$	$\int L_{\rm CO\ 1\rightarrow0}$	$L_{\rm CO\ 2\rightarrow1}$	$L_{\rm HCN\ 1\rightarrow0}$	$L_{\rm CS\ 3\rightarrow2}$	$L_{\rm FIR}$
NGC 0034	2	2.3 ± 0.1	–	0.28 ± 0.01	0.56 ± 0.07	< 0.1	14.3
NGC 0931	1	0.08 ± 0.04	–	–	< 0.1	–	2.1
NGC 1068	2	0.42 ± 0.01	$\gtrsim 3.8^a/23 \pm 8^b$	–	0.09 ± 0.01	–	7.4
NGC 1365	2	1.5 ± 0.1	5.3^c	0.48	0.16 ± 0.03	0.063 ± 0.006	6.8
NGC 1667	2	1.18 ± 0.08	–	–	0.45 ± 0.06	–	4.2
UGC 03374	1	0.40 ± 0.04	–	–	< 0.05	–	2.9
NGC 2273	2	0.041 ± 0.003	0.38 ± 0.07^b	–	0.008 ± 0.004	–	0.66
Mrk 10	1	0.3 ± 0.1	–	–	< 0.1	–	2.7
NGC 4593	1	0.08 ± 0.02	–	0.025 ± 0.003	–	–	0.79
Mrk 231	1	6.0 ± 0.6	5^d	–	1.0 ± 0.2	–	128
NGC 5033	2	0.093 ± 0.006	10 ± 3^b	–	0.014 ± 0.002	–	0.53
Mrk 273	2	2.4 ± 0.4	–	–	2.4 ± 0.8	–	73
NGC 5135	2	2.0 ± 0.1	–	0.69 ± 0.02	0.11 ± 0.01	< 0.06	9.0
NGC 5347	2	0.03 ± 0.01	–	–	< 0.01	–	0.28
NGC 5548	1	0.4 ± 0.2	–	0.29 ± 0.02	–	–	0.86
Arp 220	2	2.6 ± 0.1	–	–	0.4 ± 0.2	–	84
NGC 6814	1	0.118 ± 0.002	0.38 ± 0.06^b	0.015	0.011 ± 0.002	< 0.01	0.66
NGC 7130	2	2.6 ± 0.2	–	0.96	0.16 ± 0.02	< 0.03	11.9
NGC 7172	2	0.23 ± 0.04	–	0.19 ± 0.01	–	–	1.2
NGC 7469	1	2.00 ± 0.09	1.9 ± 0.3^b	–	0.25 ± 0.07	–	18.2

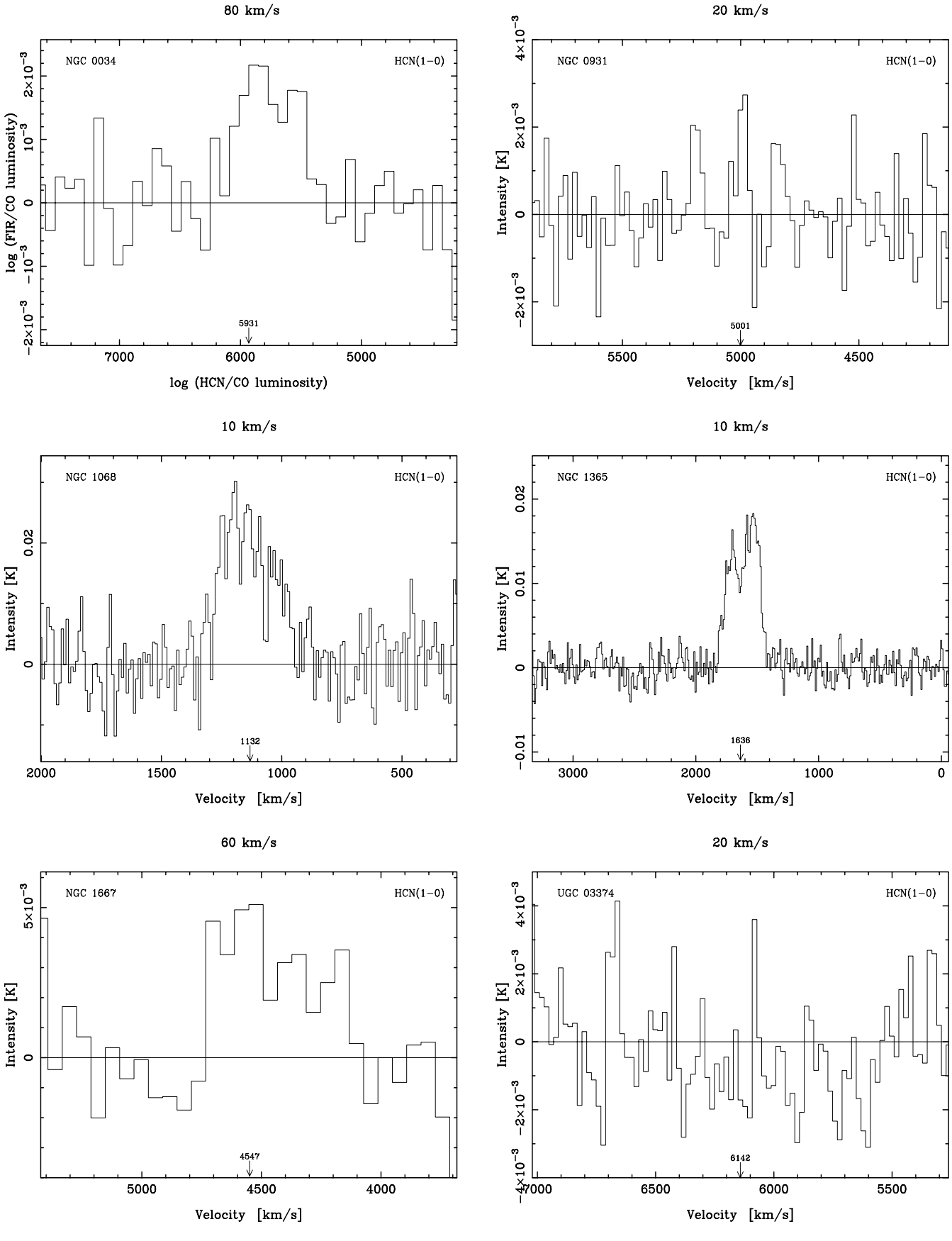

Fig. 3. The HCN $J = 1 \rightarrow 0$ results

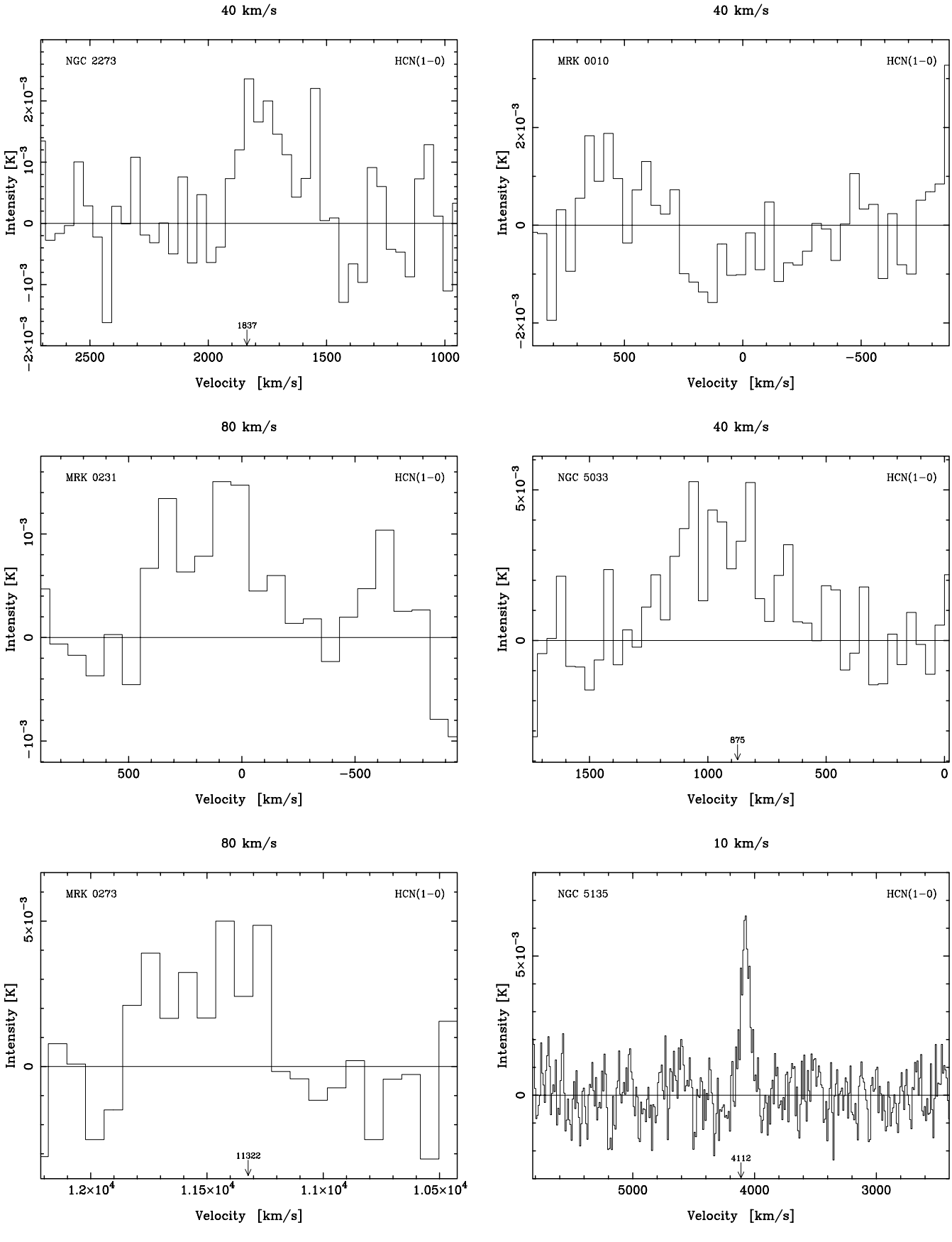

Fig. 3. continued

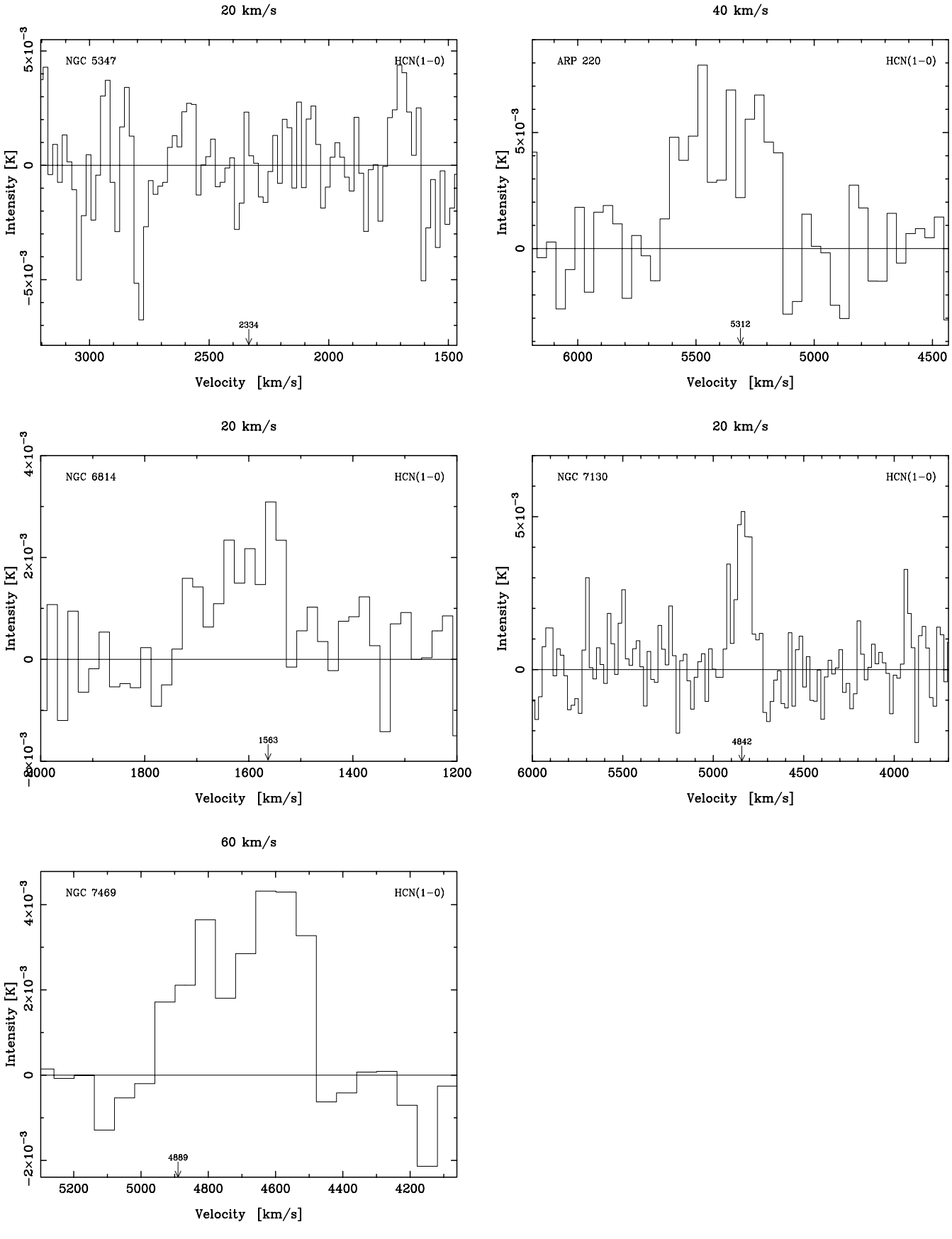

Fig. 3. continued

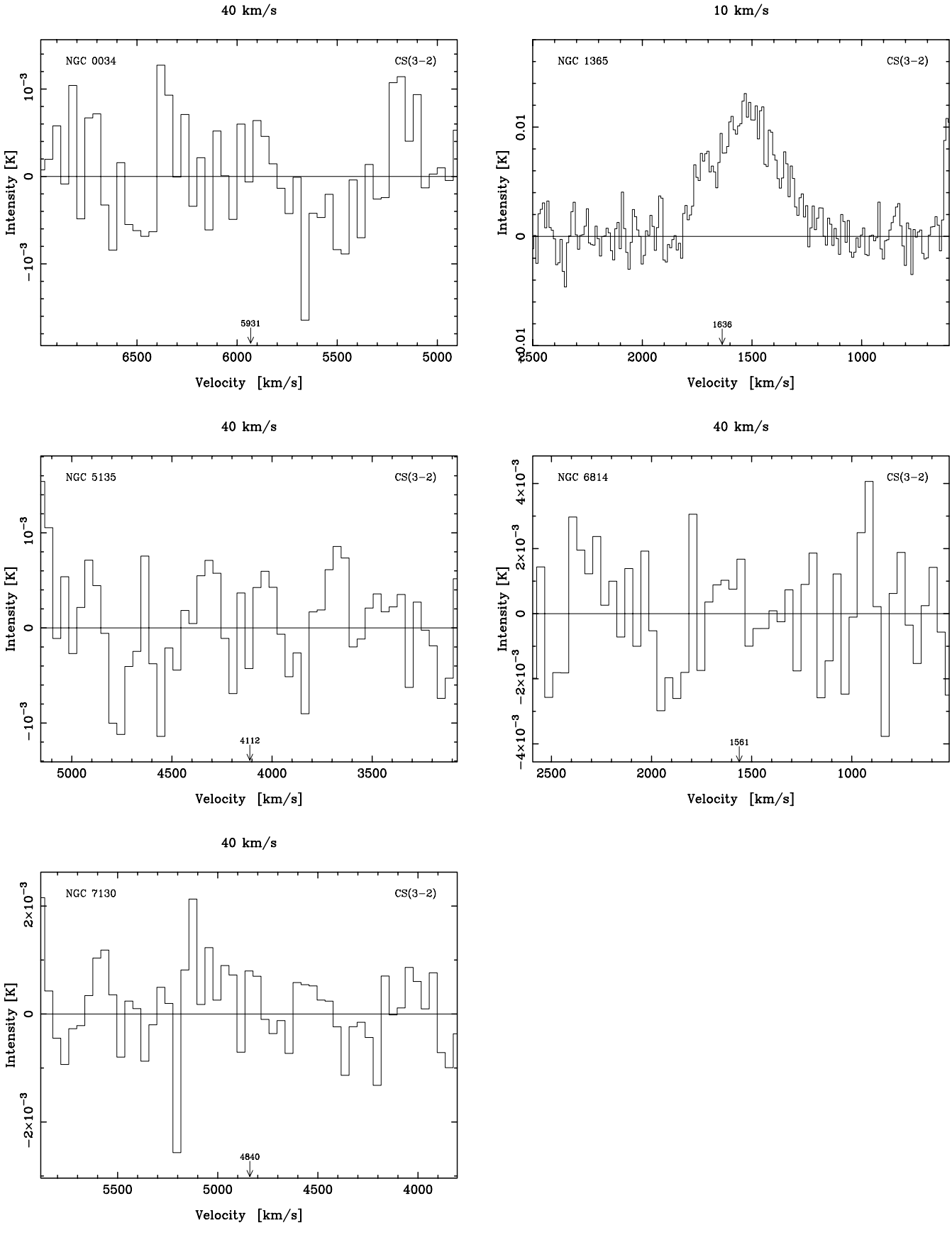

Fig. 4. The CS $J = 3 \rightarrow 2$ results

Table 4. The approximate observed CO $1 \rightarrow 0$/HCN $1 \rightarrow 0$ luminosity ratios

Galaxy	Sy	$\frac{L_{\rm CO}}{L_{\rm HCN}}$	Published intensity ratios
NGC 0034	2	4	–
NGC 0931	1	$\gtrsim 1$	–
NGC 1068	2	5	9 (Helfer & Blitz 1993)
NGC 1365	2	9	–
NGC 1667	2	3	–
UGC 03374	1	$\gtrsim 4$	–
NGC 2273	2	5	–
Mrk 10	1	$\gtrsim 3$	–
Mrk 231	1	6	4.2 (SDR92)
NGC 5033	2	7	–
Mrk 273	2	1	–
NGC 5135	2	18	–
NGC 5347	2	$\gtrsim 3$	–
Arp 220	2	7	8 (SDR92)
NGC 6814	1	11	–
NGC 7130	2	16	13 (Aalto et al. 1995)
NGC 7469	1	4	10 (Bryant 1997)

$\approx$ 10 kpc at OSO)[5], beyond which there is expected to exist little molecular gas (Maiolino et al. 1997). Plotting $\log L_{\rm CO}$ against $\log L_{\rm HCN}$ for all of the sample, however, Fig. 5, we see that we obtain the same linear relationship between the CO[6] and HCN luminosities. From

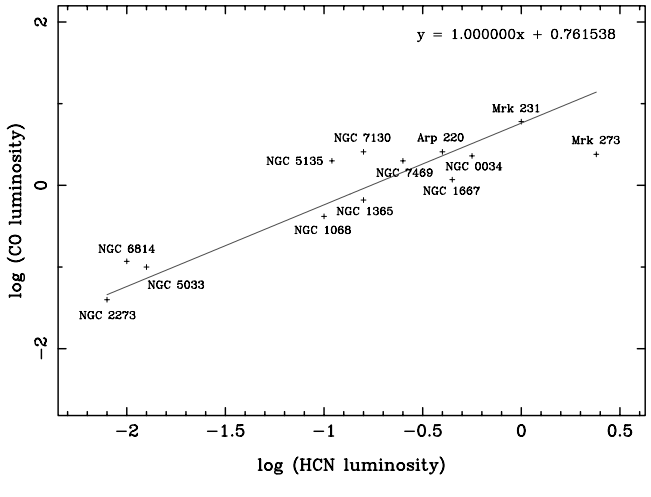

Fig. 5. $\log L_{\rm CO}$ versus $\log L_{\rm HCN}$ (units as in Table 3, i.e. $\times 10^3$ K km s^{-1} kpc^2) for all the detections. From these we obtain a ratio of $L_{\rm CO}/L_{\rm HCN} = 6^{+5}_{-3}$ and using only sources with $v \gtrsim 4000$ km s^{-1}, we obtain a ratio of $L_{\rm CO}/L_{\rm HCN} = 6^{+7}_{-3}$

the intercept of the log plot, we estimate the $L_{\rm HCN}$ to $L_{\rm CO}$ ratio for the sample to be similar to the value determined for the ULIRGs (SDR92; Bryant 1997). It is interesting that this relationship holds true for both the distant ($v \gtrsim 4000$ km s^{-1}) and near-by ($v \lesssim 4000$ km s^{-1}) sources, as it implies that the global CO/HCN luminosity ratio for distant sources $\approx$ the central ratio for near-by sources ≈ 6. If we plot the global CO values from the literature, Table 3, against the observed HCN luminosities we obtain a ratio of $L_{\rm CO}/L_{\rm HCN} = 17^{+15}_{-8}$.

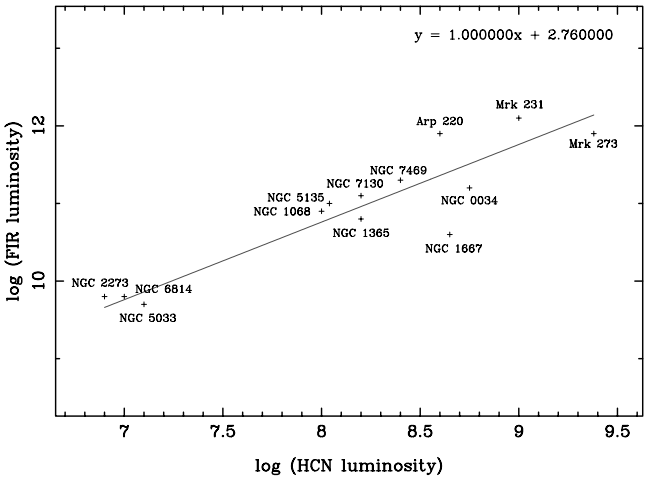

Fig. 6. $\log L_{\rm FIR}$ [$L_\odot$] versus $\log L_{\rm HCN}$ [K km s^{-1} pc^2] for all the detections

In order to determine the far infrared/HCN luminosity correlation, i.e. compare our results with those of SDR92, we plotted $\log L_{\rm FIR}$ against $\log L_{\rm HCN}$, for all[7] of the sources, Fig. 6. Here we see that we again obtain a fair linear relationship between the FIR and the HCN luminosities and from this we determine $L_{\rm FIR} \approx 600^{+600}_{-300}\ L_{\rm HCN}\ L_\odot$(K km s^{-1} pc^2)$^{-1}$.

4. Discussion

We find a mean global $L_{\rm HCN}/L_{\rm CO}$ ratio of 1/6 for our sample of Seyfert galaxies, which is similar to what SDR92 find for a set of five ULIRGs. From the HCN/CO luminosity plot it is somewhat surprising that the luminosity ratio of 1/6 holds for all the detections (Fig. 5), since we expected a larger contribution from the disk in the distant sources ($v \gtrsim 4000$ km s^{-1}), resulting in a lower $L_{\rm HCN}/L_{\rm CO}$ compared to the near-by galaxies. Typically the HCN/CO ratio in the disks of galaxies is greater than 40 (e.g. Helfer & Blitz 1993; Kuno et al. 1995), however, here both near-by and distant sources obey the same $L_{\rm CO}$

[5] Assuming a Hubble parameter of $H_0 = 75$ km s^{-1} Mpc^{-1}. This value is used in all other size estimates throughout the paper.

[6] From now on, unless otherwise stated, when CO is written it refers to the $1 \rightarrow 0$ transition.

[7] Since the HCN may possibly be more confined than the CO; within 1 kpc (the HPBW at $v \approx 1000$ km s^{-1}) (Downes et al. 1992; Nguyen et al. 1992; Henkel et al. 1994; Tacconi et al. 1996).

to $L_{\rm HCN}$ correlation, and so this may (partly) be an effect of a highly centralised molecular emission. From interferometric studies of the CO distribution we know this to be true for FIR luminous objects such as Mrk 231, Mrk 273, Arp 220 and NGC 7469, but also less FIR bright galaxies such as NGC 0034, NGC 1667 and NGC 7130 have very bright HCN with respect to their CO emission. It is possible that we are missing CO emission at radii greater than 6 kpc, thus getting an incorrect global $L_{\rm HCN}/L_{\rm CO}$ ratio, but the more likely explanation is that the CO emission is also highly concentrated in these galaxies. This confinement of the CO is another similarity between our sample and ULIRGs (Scoville et al. 1991), as opposed to normal spirals where the HCN is much more centralised than the CO (Helfer & Blitz 1993).

Comparing the global with our measured CO luminosities of the near-by sample (Table 3), it appears that the CO extends well beyond ≈ 3 kpc in the near-by sample (based on NGC 2273), while the HCN is expected to be confined to within 1 kpc (Sect. 3), leading us to believe that we have sampled the majority of the HCN in the near-by galaxies. Why should we have different CO distributions for the distant and near-by galaxies? Examining the FIR luminosities (Table 3), the mean values of the luminosities are $L_{\rm FIR} \approx 30\ 10^{10}\ L_{\odot}$ for $v > 4000$ km s^{-1} and $L_{\rm FIR} \approx 2\ 10^{10}\ L_{\odot}$ for $v < 4000$ km s^{-1}. In the case of ULIRGs, the high FIR luminosity is an indicator of a high CO concentration (Bryant 1997), and so perhaps there exists a selection effect at play, in which our distant sources comprise mainly of galaxies suffering from little CO contamination in the galactic disk.

The FIR/HCN luminosity plot, Fig. 6, shows a similar correlation to that of SDR92, which holds over a large range[8] of $L_{\rm FIR}$ and $L_{\rm HCN}$. It appears that, in our Seyfert sample, as in the ULIRGs, the FIR to HCN luminosity is similar to that of normal spiral galaxies, i.e.

$$\frac{L_{\rm FIR}}{L_{\rm HCN}}\ (\text{Seyferts}) \approx \frac{L_{\rm FIR}}{L_{\rm HCN}}\ (\text{normal spirals}) \qquad (1)$$

and since normal spirals have $L_{\rm HCN}/L_{\rm CO} \approx 1/80$ (SDR92), from previously

$$\frac{L_{\rm HCN}}{L_{\rm CO}}\ (\text{distant Seyferts}) \approx 10\frac{L_{\rm HCN}}{L_{\rm CO}}\ (\text{normal spirals}), \qquad (2)$$

and combining these equation gives

$$\frac{L_{\rm FIR}}{L_{\rm CO}}\ (\text{distant Seyferts}) \approx 10\frac{\rm L_{FIR}}{L_{\rm CO}}\ (\text{normal spirals}). \qquad (3)$$

As a further check, in order to account for the distances and the extents in our sample, as SDR92, we plotted $L_{\rm FIR}/L_{\rm CO}$ against $L_{\rm HCN}/L_{\rm CO}$, Fig. 7.

From this we can see that the normalisation does not significantly alter the linear fit, although three of the sample deviate further from the line. In any case, from the fit we also find

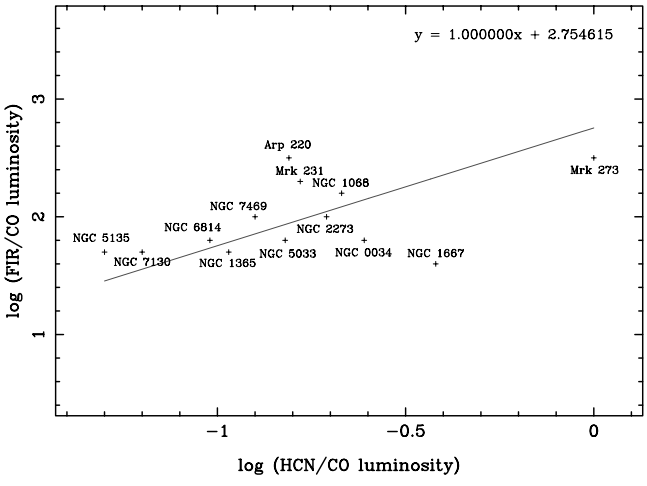

Fig. 7. $\log L_{\rm FIR}$ $[L_{\odot}({\rm K\ km\ s^{-1}\ pc^2})^{-1}]$ versus $\log L_{\rm HCN}$ normalised by the CO luminosity for all the detections [no units]

$L_{\rm FIR} \approx 600 L_{\rm HCN}\ L_{\odot}({\rm K\ km\ s^{-1}\ pc^2})^{-1}$ (normalised by the CO luminosity)[9] which again agrees well with the result of SDR92 ($L_{\rm FIR} \approx 750 L_{\rm HCN}\ L_{\odot}({\rm K\ km\ s^{-1}\ pc^2})^{-1}$).

With regard to what these results entail, we interpret the high $L_{\rm HCN}/L_{\rm CO}$ ratio in our sample of Seyferts as largely an effect of a high degree of central concentration of the gas[10]. The steep central potential and high gas surface densities result in large gas pressures which could force the bulk of the molecular mass to reside in high density gas. This should be true regardless of what activity dominates the FIR emission from the galaxy. SDR92 suggest that the $L_{\rm HCN}/L_{\rm FIR}$ correlation means that the HCN emission traces star forming cores, which are responsible for the IR emission, i.e. the ULIRGs are powered by star-bursts. For several of the Seyferts in our sample, however, at least 50% of the FIR emission may come from the AGN activity, even if a star-burst also contributes to the total luminosity: Kohno et al. (1999) suggest that Seyferts with jets have particularly bright HCN emission and that the dense gas, which is a component of a large-scale obscuration[11] confines the jet (Antonucci & Miller 1985; Wilson et al. 1988; Tadhunter & Tsvetanov 1989; Wilson & Tsvetanov 1994; Baker & Scoville 1998). Also, Bryant (1997); Kohno et al. (1999) discuss the connection between very high HCN/CO ratios and these nuclei and point out that Seyfert nuclei are associated with the lowest published HCN/CO ratios

[8] From normal spirals to ULIRGs (SDR92; Helfer & Blitz 1993).

[9] We achieve the same value using only galaxies with $v \gtrsim 4000$ km s^{-1}, thus again indicating that the CO may be centralised.

[10] For example, in NGC 1068 the HCN/CO intensity ratio is 0.6 in the central few hundred pc (Helfer & Blitz 1995) cf. ≈ 0.2 within 1.2 kpc (this work) and 0.1 out to 2.2 kpc (Helfer & Blitz 1993).

[11] E.g. Shlosman, Begelman & Frank (1990); Friedli & Martinet (1993); Shaw et al. (1993); Wilson & Tsvetanov (1994); Maiolino & Rieke (1995); Fosbury et al. (1999); Conway (1999); Curran (2000a).

so far. The only similarity between these objects is that they host broad-line AGN, and similarly, in our sample, NGC 1667 and Mrk 273 both have extremely bright HCN with respect to CO, yet they differ by over an order of magnitude in their FIR luminosities.

An $L_{\rm HCN}/L_{\rm CO}$ ratio of 1/6 is at the lower end of what is typically found even for galactic nuclei. For near-by galaxies, standard HCN/CO ratios appear to range between 1/15 and 1/5 on scales smaller than a kiloparsec (e.g. Helfer & Blitz 1995; Aalto et al. 1995), and so a high degree of gas concentration may not be a sufficient explanation for the high ratio we observe. The "extra" bright HCN emission may be an additional effect of extreme gas excitation and/or unusual abundance effects.

Heckman et al. (1989) state that the CO and far infrared properties differ between the two Seyfert classes, although Seyferts as a class exhibit similar $L_{\rm CO}$ to $L_{\rm FIR}$ ratios to non-Seyferts. In order to test this, we plot the log of the $L_{\rm CO}/L_{\rm FIR}$ ratio versus the log of $L_{\rm FIR}$ (Table 3), and find that, not unexpectedly, all of our detections lie in the same range as Fig. 6 of Heckman et al. (1989), Fig. 8. From these results we calculate the mean ratio, at a 90% confidence level, to be

$$\log\left(\frac{L_{\rm CO}}{L_{\rm FIR}}\right) = -8.0 \pm 0.2 \text{ for } v \gtrsim 4000 \text{ km s}^{-1} \text{ and,} \quad (4)$$

$$\log\left(\frac{L_{\rm CO}}{L_{\rm FIR}}\right) = -8.0 \pm 0.1 \text{ for all the detections.} \quad (5)$$

cf. −7.76 for Seyferts and −7.84 for non-Seyferts (Heckman et al. 1989).

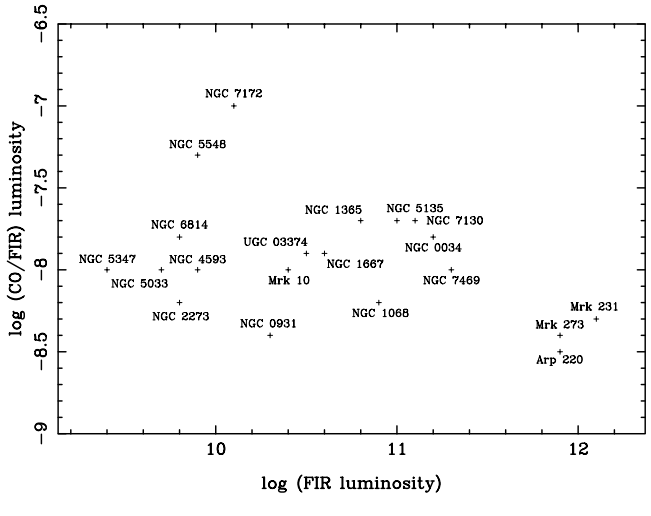

Fig. 8. $\log L_{\rm CO}/L_{\rm FIR}$ [K km s^{-1} kpc^2 $L_\odot^{-1}$] versus $\log L_{\rm FIR}$ [$L_\odot$]

This is the same range over which normal spiral galaxies are distributed (Young et al. 1984; Sanders & Mirabel 1985; Stark et al. 1986; Young et al. 1986). If we refer to Fig. 6c of Sanders & Mirabel (1996), our sample is located at around[12] $L_{\rm FIR} \lesssim 10^{11}\ L_\odot \approx 20M({\rm H_2})\ M_\odot$, cf. $L_{\rm FIR} < 10^{11}\ L_\odot \approx 10M({\rm H_2})\ M_\odot$ for normal spirals[13] and $L_{\rm FIR} \gtrsim 10^{11}\ L_\odot \approx 50M({\rm H_2})\ M_\odot$ for star-burst galaxies. So we find that for similar values of $L_{\rm FIR}$, that our sample has about double the $L_{\rm FIR}/L_{\rm CO}$ ratio of normal spiral galaxies and a similar ratio to the more moderate star-burst galaxies ($L_{\rm FIR} \sim 10^{11} - 10^{12}\ L_\odot$)[14].

As seen from Fig. 8 and Fig. 6c of Sanders & Mirabel (1996), the Seyfert sample follows the same trend for $L_{\rm CO}/L_{\rm FIR}$ to decrease over an order of magnitude as defined by normal spirals to ULIRGs, with the Seyferts being located in between these two extremes. This result could be caused by either:

1. The FIR luminosity arising from young stars, in which case the HCN would be tracing dense star-forming cloud cores[15].
2. The FIR luminosity arising from something other, i.e. an AGN.

In the first case we would expect the $L_{\rm FIR}/L_{\rm HCN}$ ratio to be fairly independent of the FIR luminosity of the galaxy and in the latter case we would expect $L_{\rm FIR}/L_{\rm HCN}$ to increase, i.e. a further FIR contribution in addition to that from star formation coming into play. Plotting the $L_{\rm HCN}/L_{\rm FIR}$ ratio versus $L_{\rm FIR}$ (in a similar manner to Fig. 8), Fig. 9, we see that the HCN/FIR ratio may well decrease with the FIR luminosity[16] thus indicating that the latter scenario may be the case, although with these statistics this is far from conclusive. In support of the non-AGN argument, a constant (on average) value of $L_{\rm HCN}/L_{\rm FIR}$ may be feasible (although the least squares linear fit does give a non-zero gradient, Fig. 9).

This is supported by Figs. 6 and 7 where a simple line does provide a good fit; a decreasing $L_{\rm HCN}/L_{\rm FIR}$ ratio would demand a (slight on a log−log plot) curve in these figures. Also from Figs. 6 and 7, there appears to be no FIR to HCN excess cf. normal gas rich galaxies and ULIRGs (SDR92), although their fit may be significantly affected by the high values of $L_{\rm FIR}$ for

[12] Assuming that the molecular hydrogen mass, $M({\rm H_2})[M_\odot] = 4.6 L_{\rm CO}$ [K km s^{-1} pc^2] (Scoville & Sanders 1987).

[13] Since this ratio of $\frac{L_{\rm FIR}}{L_{\rm CO}}$ (Seyferts) $\approx 2\frac{L_{\rm FIR}}{L_{\rm CO}}$ (normal spirals) is based on the whole sample, and not just the distant FIR bright Seyferts, it is somewhat less than that determined by Eq. (3).

[14] The extreme cases; Mrk 231, Mrk 273 and Arp 220, which are located in the $L_{\rm FIR} \sim 10^{12}\ L_\odot \approx 70M({\rm H_2})\ M_\odot$ range, are also considered to be ULIRGs (e.g. SDR92; Downes & Solomon 1998).

[15] Estimating the CO 2 → 1 source sizes from the radio continuum (e.g. Allen 1992; Bajaja et al. 1995) we find that the CO emission seems to be sub-thermally excited, which would suggest a less dense cloud component in addition to that traced by the HCN. This is discussed further in Curran (2000b).

[16] Over a factor of two according to the linear fit from $L_{\rm FIR} \sim 10^{10} - 10^{12}\ L_\odot$.

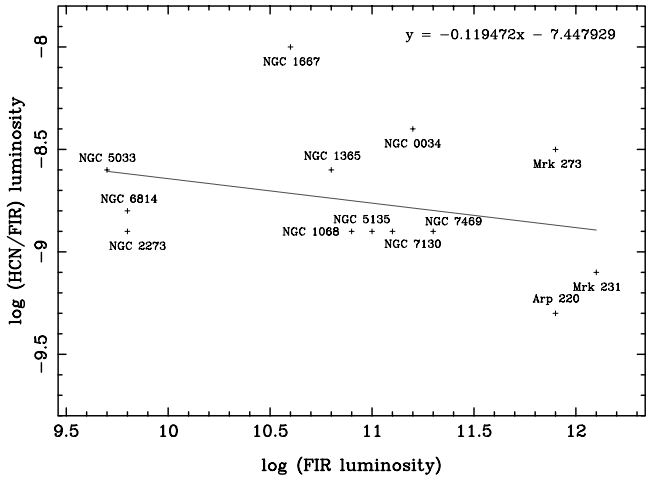

Fig. 9. $\log L_{\rm HCN}/L_{\rm FIR}$ [K km s^{-1} kpc^2 $L_\odot^{-1}$] versus $\log L_{\rm FIR}$ [$L_\odot$]. The least squares linear fit is shown

Mrk 231 and Arp 220 which are also considered to be Seyferts[17], and there does remain the possibility that the HCN may be associated with the gas obscuring the AGN rather than dense star-forming cores. The low CS 3 → 2/HCN 1 → 0 luminosity ratios (< 0.5) in the (Southern) sample may support this result (Curran 2000b).

A similar correlation for both Seyfert and star-burst galaxies is also found between $L_{\rm FIR}$ and $L_{\rm H\alpha}$ (Gu et al. 1997), and this as well as other Seyfert samples, which utilise FIR luminosities (e.g. in comparison with $L_{\rm blue}$; Whittle 1992; Gu et al. 1999 and the radio continuum; Roy et al. 1998), lead to the conclusion that the FIR flux is thermal in origin for most Seyfert galaxies.

5. Summary

We have detected CO 1 → 0 in all and HCN 1 → 0 in 13 of the 20 Seyfert galaxies observed. The detections include six new detections in HCN for NGCs 1667, 2273, 5033, Mrk 273, NGC 5135 and NGC 6814. Similar to ULIRGs, for the distant sources we find a global HCN to CO luminosity ratio of ≈ 1/6 which is an order of magnitude greater than in normal spiral galaxies and, again as in the case of ULIRGs (Scoville et al. 1991), this implies that the CO appears to be confined to the nuclear region (otherwise an even lower luminosity ratio is obtained). The $\frac{\rm CO\ 1\to0}{\rm HCN\ 1\to0}$ intensity ratios obtained are significantly lower than those in moderate infrared luminosity ($L_{\rm FIR} < 10^{11}\ L_\odot$) galaxies. Also, perhaps because of the centralisation, our sample does not appear to suffer from the same selection effect at play, due to the difficulty in detecting HCN in such distant galaxies, cf. $\frac{\rm CO\ 1\to0}{\rm HCN\ 1\to0} > 20$ at velocities $\gtrsim$ 4000 km s^{-1} for moderate infrared luminosity galaxies (Bryant 1997), although a selection effect may be responsible for the high CO/HCN ratios here.

We also find that the HCN to FIR luminosity ratio is similar to that for normal spiral galaxies through to ULIRGs. This result implies that there is no excess in the far infrared continuum (which could be due to an AGN) in our sample, although if the denser gas tracers form part of the obscuration rather than star-forming clouds, the FIR to HCN ratio would imply an additional FIR source. In any case, as the results stand there is no overwhelming evidence to invoke a contribution from an AGN.

Acknowledgements. We are grateful to the anonymous referee for his helpful comments and we would like to thank Per Bergman, Lars E.B. Johansson and the SEST and Onsala telescope operators. This research has made use of the NASA/IPAC Extragalactic Database (NED) which is operated by the Jet Propulsion Laboratory, California Institute of Technology, under contract with the National Aeronautics and Space Administration.

[17] In fact ∼ 10% of ULIRGs are considered to be type 1 Seyferts or IR QSOs (Deng et al. 1997) and up to ≈ 80% may be radio quiet AGNs (i.e. Seyferts and LINERs) (Wu et al. 1998) and up to ≈ 30% may be powered by AGNs in general (Genzel et al. 1998).

References

Aalto S., Booth R.S., Black J.H., Johansson L.E.B., 1995, A&A 300, 369
Allen R.J., 1992, ApJ 399, 573
Antonucci R.R.J., Miller J.S., 1985, ApJ 297, 621
Bajaja E., Wielebinski R., Reuter H.P., Harnett J.I., Hummel E., 1995, A&AS 114, 147
Baker A.J., Scoville N.Z., 1998, Am. Astron. Soc. Meet. 192, 3605
Begelman M.C., Blandford R.D., Rees M.J., 1984, Rev. Mod. Phys. 56, 255
Bryant P.M., Scoville N.Z., 1996, ApJ 457, 678
Bryant P.M., 1997, Ph.D. Thesis. California Institute of Technology
Conway J., 1999, HI Absorption from a Circumnuclear TORUS in the Hidden Quaser Cygnus A. In: Carilli C., Radford S., Menton K., Langston G. (eds.). Highly Redshifted Radio Lines, ASP Conf. Ser., p. 259
Curran S.J., Koribalski B., Haynes R.F., Krause M., Johansson L.E.B., 2000, A&A (in preparation)
Curran S.J., 2000a, A&A (in preparation)
Curran S.J., 2000b, Ph.D. Thesis. Chalmers University of Technology (in preparation)
Deng Z.G., Xia X.Y., Wu H., 1997, in IAU Symposia, p. 110
Downes D., Solomon P.M., 1998, ApJ 507, 615
Downes D., Radford S.J.E., Guilloteau S., et al., 1992, A&A 262, 424
Edelson R.A., 1987, ApJ 313, 651
Fosbury R.A.E., Vernet J., Villar-Martin M., et al., 1999, Optical Continuum Structure of Cygnus A. In: Best P., Lehnert M. (eds.). KNAW colloqium on: The Most Distant Radio Galaxies. Reidel, Amsterdam (in press)
Friedli D., Martinet L., 1993, A&A 277, 27
Genzel R., Lutz D., Sturm E., et al., 1998, ApJ 498, 579

Gu Q.S., Huang J.H., Su H., Shang Z.H., 1997, A&A 319, 92
Gu Q.S., Huang J.H., Ji L., 1999, Astrophys. Space Sci. 260, 389
Heckman T.M., Blitz L., Wilson A.S., Armus L., Miley G.K., 1989, ApJ 342, 735
Helfer T.T., Blitz L., 1993, ApJ 419, 86
Helfer T.T., Blitz L., 1995, ApJ 450, 90
Helfer T.T., Blitz L., 1997, ApJ 478, 233
Henkel C., Whiteoak J.B., Mauersberger R., 1994, A&A 284, 17
Kohno K., Kawabe R., Vila-Vilaró B., 1999, NMA Survey of CO and HCN Emission from Nearby Active Galaxies. In: The Proceedings of the 3rd Cologne-Zermatt Symposium, "The Physics and Chemistry of the Interstellar Medium", p. 2251
Kuno N., Nakai N., Handa T., Sofue Y., 1995, PASJ 47, 745
Lonsdale C.J., Helou G., Good J.C., Rice W., 1985, Cataloged Galaxies and Quasars Observed in the IRAS Survey. Jet Propulsion Laboratory, Pasadena
Maiolino R., Rieke G.H., 1995, ApJ 454, 95
Maiolino R., Ruiz M., Rieke G.H., Papadopoulos P., 1997, ApJ 485, 552
Meurs E.J.A., Wilson A.S., 1984, A&A 136, 227
Miyoshi M., Moran J., Herrnstein J., et al., 1995, Nat 373, 127
Nguyen Q., Jackson J.M., Henkel C., Truong B., Mauersberger R., 1992, ApJ 399, 521
Osterbrock D.E., Shaw R.A., 1988, ApJ 327, 89
Osterbrock D.E., 1981, ApJ 249, 462
Papadopoulos P.P., Seaquist E.R., 1998, ApJ 492, 521
Planesas P., Gomez-Gonzalez J., Martin-Pintado J., 1989, A&A 216, 1
Rees M.J., 1984, ARA&A 22, 471
Roy A.L., Norris R.P., Kesteven M.J., Troup E.R., Reynolds J.E., 1998, MNRAS 301, 1019
Rydbeck G., Wiklind T., Cameron M., et al., 1993, A&A 270, L13
Sanders D.B., Mirabel I.F., 1985, ApJ 298, L31
Sanders D.B., Mirabel I.F., 1996, Ann. Rev. Astr. Ap. 34, 749
Sanders D.B., Scoville N.Z., Young J.S., et al., 1986, ApJ 305, L45
Sandqvist A., Jörsäter S., Lindblad P., 1995, A&A 295, 585
Scoville N.Z., Sanders D.B., 1987, H_2 in the Galaxy. In: Hollenbach D.J., Jr. H.A.T. (eds.), Interstellar Processes. Reidel, Dordrecht, p. 21
Scoville N.Z., Sargent A.I., Sanders D.B., Soifer B.T., 1991, ApJ 366, L5
Shaw M.A., Combes F., Axon D.J., Wright G.S., 1993, A&A 273, 31
Shlosman I., Begelman M.C., Frank J., 1990, Nat 345, 679
Soifer B.T., Rowan-Robinson M., Houck J.R., et al., 1984, ApJ 278, L71
Solomon P.M., Sage L.J., 1988, ApJ 334, 613
Solomon P.M., Downes D., Radford S.J.E., 1992, ApJ 387, L55
Stark A.A., Knapp G.R., Bally J., et al., 1986, ApJ 310, 660
Tacconi L.J., Genzel R., Blietz M., et al., 1994, ApJ 426, L77
Tacconi L.J., Gallimore J.F., Schinnerer E., Genzel R., Downes D., 1996, BAAS 189, 906
Tadhunter C., Tsvetanov Z., 1989, Nat 341, 422
Whittle M., 1992, ApJ 387, 121
Wilson A.S., Tsvetanov Z.I., 1994, AJ 107, 1227
Wilson A.S., Ward M.J., Haniff C.A., 1988, ApJ 334, 121
Wu H., Zou Z.L., Xia X.Y., Deng Z.G., 1998, A&AS 132, 181
Young J.S., Kenney J., Lord S.D., Schloerb F.P., 1984, ApJ 287, L65
Young J.S., Schloerb F.P., Kenney J.D., Lord S.D., 1986, ApJ 304, 443
Young J.S., Xie S., Tacconi L., et al., 1995, ApJS 98, 219